Electronic Supplementary Material (ESI) for Journal of Materials Chemistry C.

Supporting Information for

Centimeter-scale growth of high-quality In_2Se_3 film for transparent, flexible and high performance photodetectors

Z. Q. Zheng, J. D. Yao and G. W. Yang

State Key Laboratory of Optoelectronic Materials and Technologies, Nanotechnology Research Center, School of Materials Science & Engineering, Sun Yat-sen University, Guangzhou 510275, Guangdong, P. R. China.

Table S1. Summary of performance parameters of recently developed 2D material-based photodetectors

Device (substrate) (Bandgap in eV)	Fabrication method	Measurement condition	Responsivity (A/W)	EQE (%)	Spectral window	D* (Jones)	Physical characteristic	Ref.
1L MoS_2 (on SiO_2/Si) (1.8, DB)	Mechanical exfoliation	520 nm $V_{ds} = 5$ V	1.17	280	Visible-NIR	$1.5 * 10^7$	Rigid	1
1L MoS_2 (on SiO_2/Si) (1.8, DB)	Mechanical exfoliation	$V_g = 50$ V $V_{ds} = 1$ V	$7.5*10^{-3}$	-	Visible	-	Rigid	2
ML MoS_2 (on SiO_2/Si) (1.2, IB)	Mechanical exfoliation	633 nm $V_g = 3$ V $V_{ds} = 1$ V	0.12	-	Visible-NIR	$5*10^7$--10^{11}	Rigid	3
Graphene (on SiO_2/Si) (gapless)	Mechanical exfoliation	1550 nm $V_g = 80$ V	$5*10^{-4}$	6-16	UV-IR	-	Rigid	4
FL GaSe (on SiO_2/Si) (2.1, IB)	Mechanical exfoliation	254 nm $V_{ds} = 5$ V	2.8	1367	UV	-	Rigid	5
ML WS_2 (on SiO_2/Si) (1.1, IB)	PLD	635 nm $V_{ds} = 9$ V	0.51	137	UV-NIR	$2.7*10^9$	Rigid	6
1L $MoSe_2$ (on SiO_2/Si) (1.56, DB)	CVD	532 nm $V_{ds} = 10$ V	$13*10^{-3}$	-	Visible	-	Rigid	7
1L WSe_2 (on SiO_2/Si) (1.62, DB)	CVD	532 nm $V_{ds} = 5$ V	3.717	860	UV-Visible	-	Rigid	8
FL GaS (on SiO_2/Si) (3.05, IB)	CVD	254 nm $V_{ds} = 2$ V	4.2	2050	UV-Visible	10^{10}--10^{14}	Rigid	9
FL InSe (on SiO_2/Si) (1.3, DB)	CVD	450 nm $V_{ds} = 10$ V	12.3	3389	Visible-NIR	$1.07*10^{11}$	Rigid	10
MoS_2/h-BN (on SiO_2/Si)	Mechanical exfoliation	500 nm $V_{ds} = 1.5$ V	5.07	1200	Visible	$3*10^{10}$	rigid	11
ML In_2Se_3 (on SiO_2/Si) (1.3, DB)	Mechanical exfoliation	300 nm $V_{ds} = 5$ V	395	163000	UV-Visible	$2.26*10^{12}$	Rigid	12

FL In_2Se_3 **(on SiO_2/Si)** **(1.26, DB)**	epitaxy	Visible light V_{ds} = 0.1 V	2.5	-	Visible	-	Rigid	13
ML In_2Se_3 **(on SiO_2/Si)**	epitaxy	Visible light V_{ds} = 5 V	7.2	-	Visible	-	Rigid	14
FL $Pb_{1-x}Sn_xSe$ **(on mica)** **(0.43, -)**	CVD	473 nm V_{ds} = 2 V	5.95	-	UV-NIR	-	Flexible	15
FL InSe **(on PET)** **(1.3, DB)**	CVD	633 nm V_{ds} = 10 V	3.9	764	Visible-NIR	$5.47*10^{10}$	Flexible	10
FL GaS **(on PET)** **(3.05, IB)**	CVD	254 nm V_{ds} = 2 V	19.2	9371	UV	-	Flexible	9
FL GaTe **(on PET)** **(1.7, DB)**	CVD	473 nm V_{ds} = 5 V	0.03	8	UV-Visible	-	Flexible	16
GaSe crystals **(on mica)** **(2.1, IB)**	Epitaxy	white light V_{ds} = 10 V	0.03	-	Visible	-	Flexible, Transparent	17
ML In_2Se_3 **(on special PI)** **(1.154, DB)**	**PLD**	**532nm** **V_{ds} = 5 V**	**20.5**	**4784**	**UV-NIR**	**$6.02*10^{11}$**	**Flexible, Transparent**	**ours**
ML In_2Se_3 **(normal PI)** **(1.154, DB)**	**PLD**	**532nm** **V_{ds} = 5 V**	**45.2**	**10558**	**UV-NIR**	**$1.6*10^{12}$**	**Flexible**	**ours**
ML In_2Se_3 **(on sapphire)** **(1154, DB)**	**PLD**	**532nm** **V_{ds} = 5 V**	**27.9**	**6525**	**UV-NIR**	**$4.88*10^{11}$**	**Transparent**	**ours**
ML In_2Se_3 **(on SiO_2/Si)** **(1.154, DB)**	**PLD**	**532nm** **V_{ds} = 5 V**	**22.96**	**5366**	**UV-NIR**	**$5.13*10^{11}$**	**Rigid**	**ours**

DB and IB represent the direct and indirect band gaps, respectively. 1L, FL and ML mean monolayer, few-layer and multilayer, respectively.

Figure S1. Size distribution histogram of the as-prepared In_2Se_3 film and corresponding Gaussian fitting curve of the grain size, which eveals that the average diameter of grain size of the as-prepared In_2Se_3 film is 34.01 nm. SD represents standard deviation.

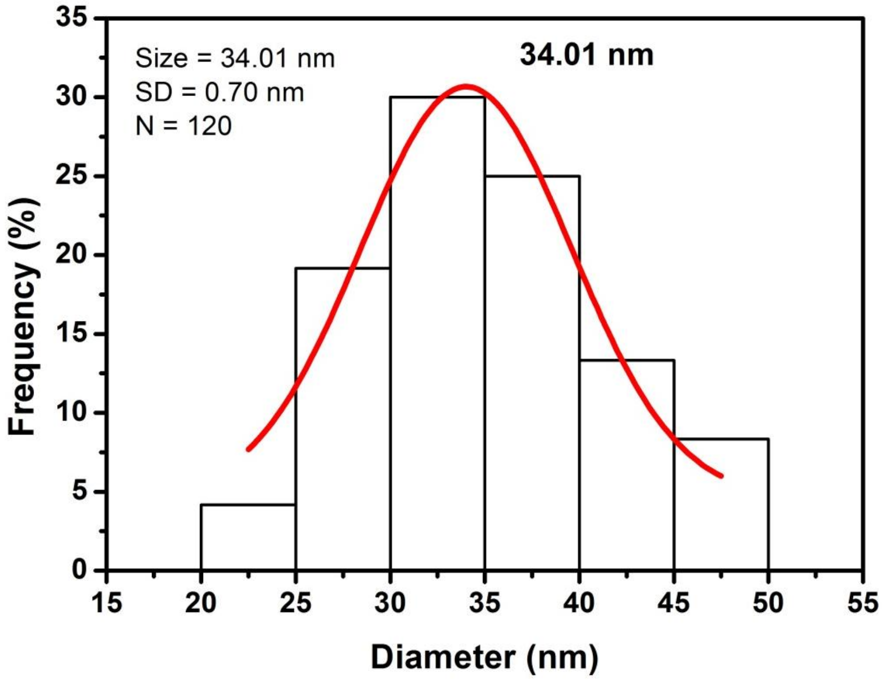

Figure S2. (a) Optical image of the In_2Se_3 sample deposited on PI substrate, in which many scratches were made with a plastic sheet for AFM measurements. (b) AFM image at the edge of a scratch in (a). The corresponding height profiles along the red dotted line and blue dotted line are demonstrated in (c) and (d), respectively. The thickness of the In_2Se_3 sample is deduced to be ~22.9 nm.

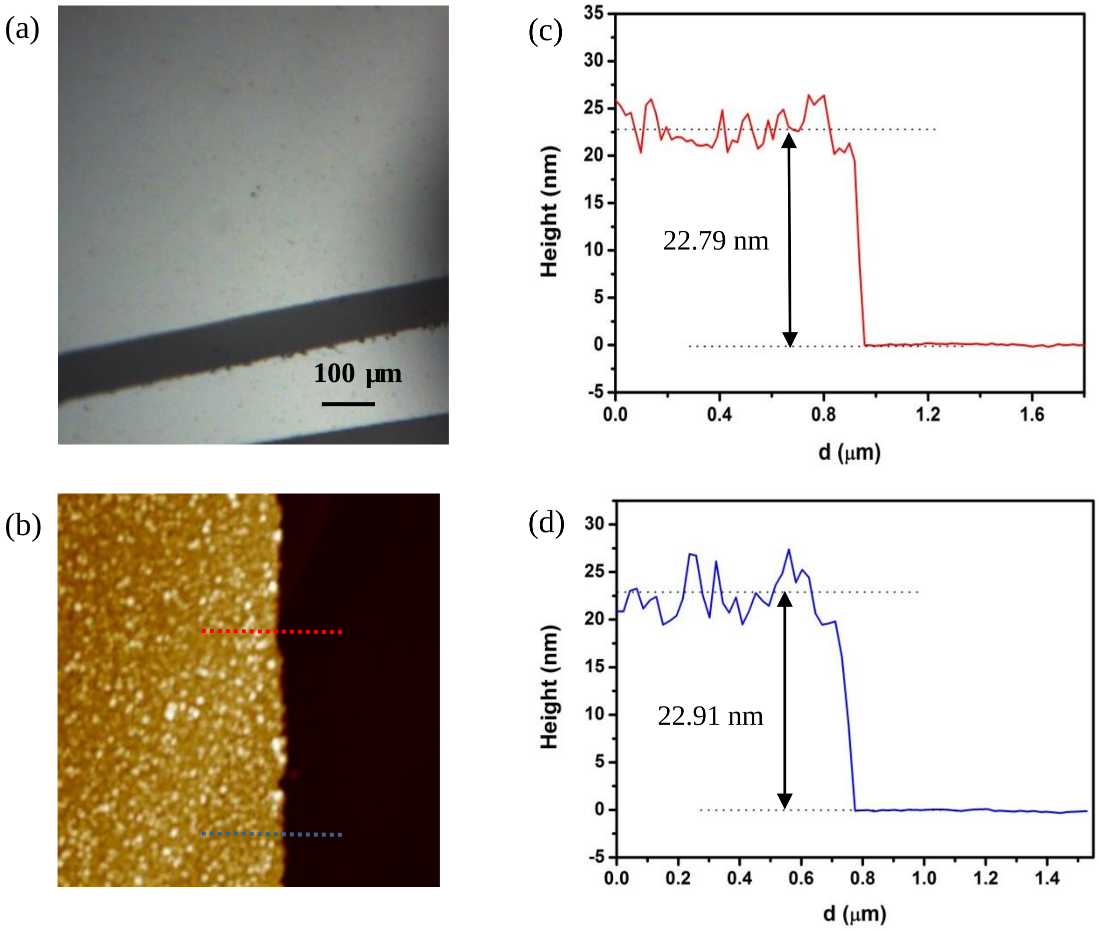

Figure S3. Raman spectrum of the as-prepared In_2Se_3 film.

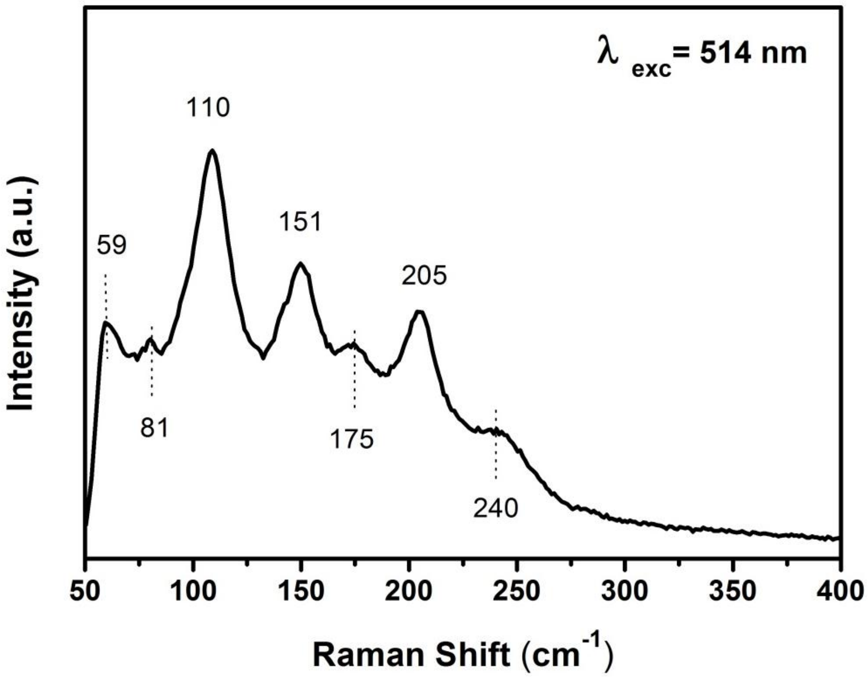

Figure S4. (a) UV-Vis-NIR diffuses reflectance absorption spectrum of the In_2Se_3 film and (b) the corresponding Tauc plot, which presents a direct bandgap of 1.154 eV for the as-prepared In_2Se_3 film.

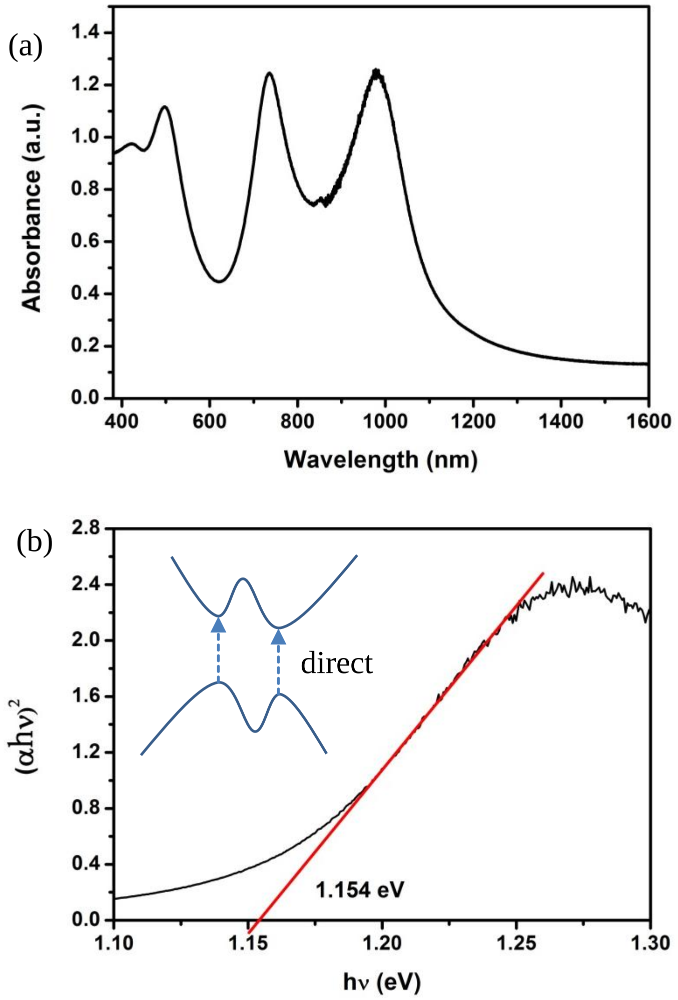

Figure S5. Voltage dependence photoresponse at different bias voltages Vds. (a) Photocurrent under 532 nm light illumination with power density of 20 mW/cm^2 as a function of bias voltage, showing a linear dependence on the bias voltage. (b) Time dependence switching behavior at different bias voltages V_{ds} from 0.2 to 5 V. Power density: 532 nm and 20 mW/cm2. (c) The working principle of bias voltage dependence photoresponse.

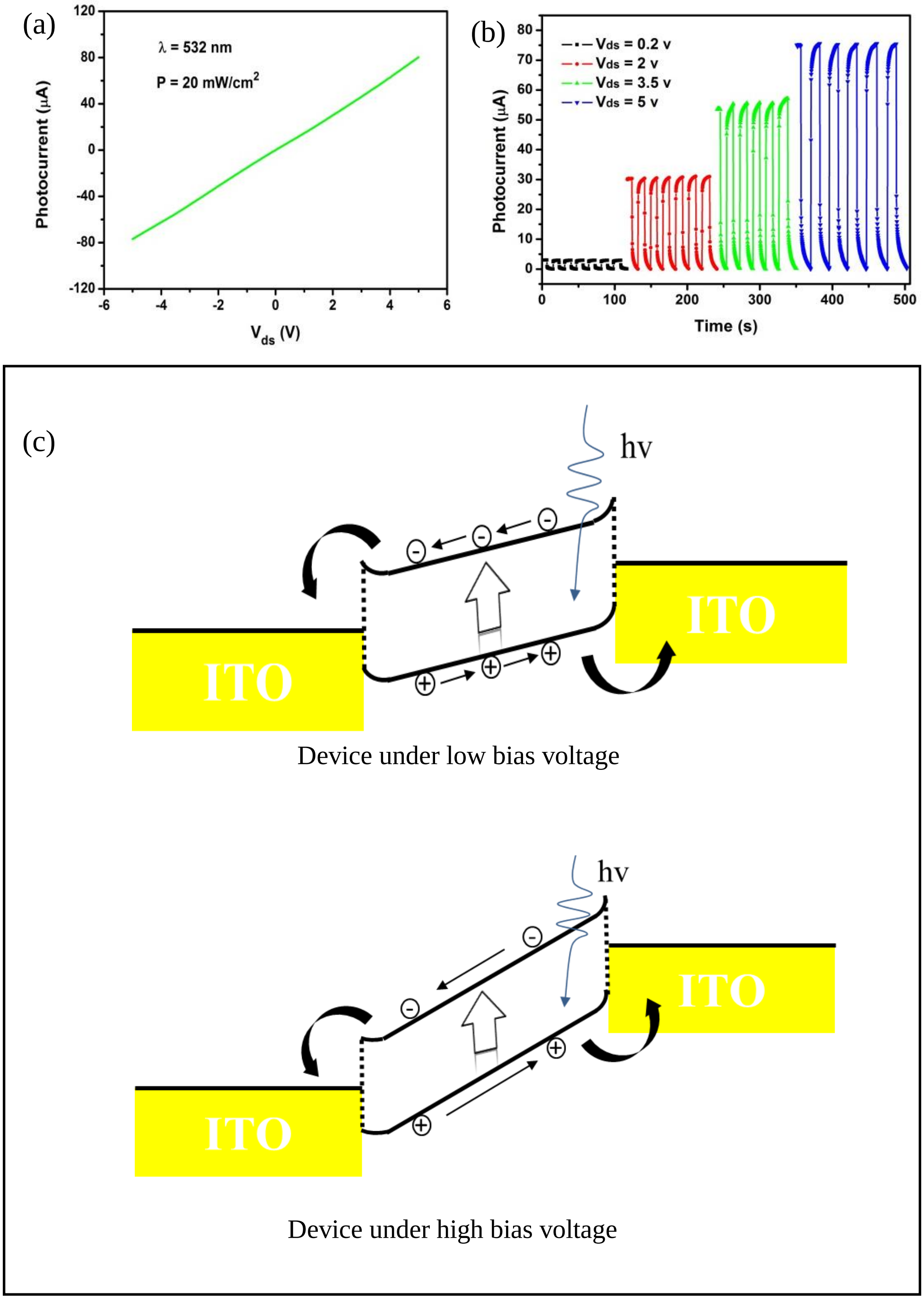

Figure S6. Transmittance and responsibility evolved with the thickness of the In_2Se_3 active layer.

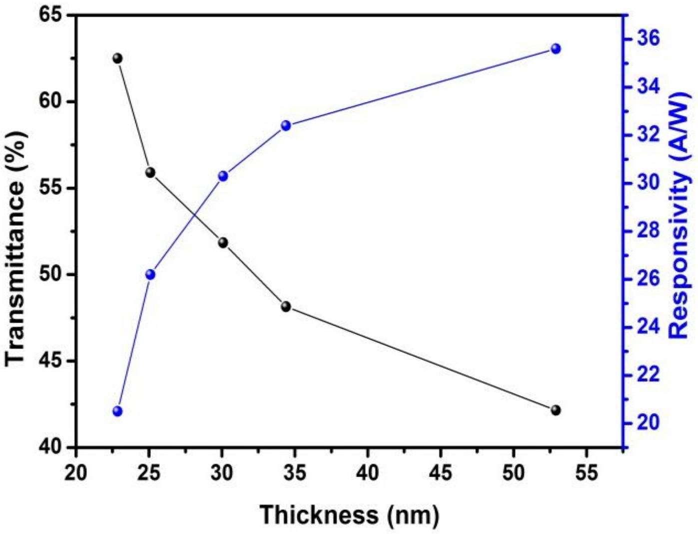

Figure S7. Photoswitching curves of the device before and after exposing to ambient environment for a month.

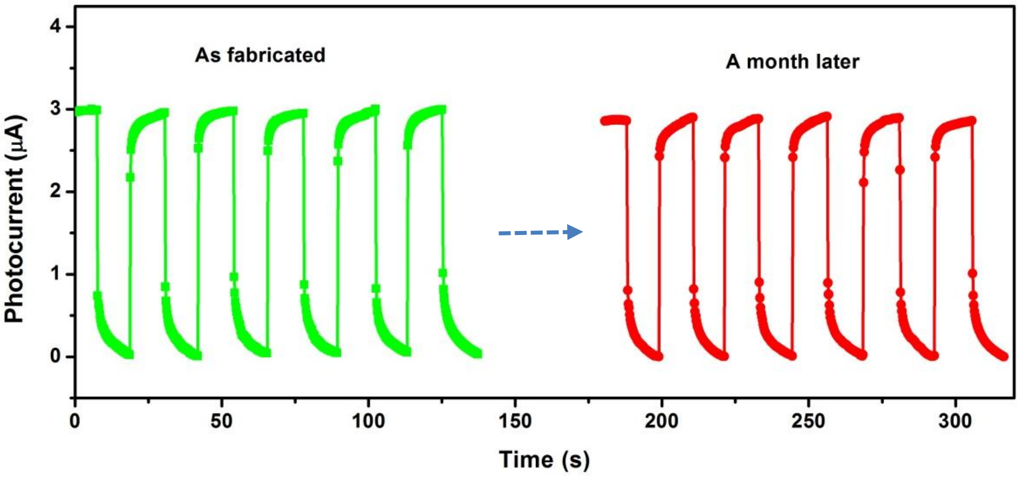

Figure S8. Greater details depict the transient current characteristic for this device: (a) rise, (b) decay. Here, the time interval between each point is 8.2 ms, and the rise/fall time was defined as the current increased/decreased from 0/100% to 80/20% of the stable current.

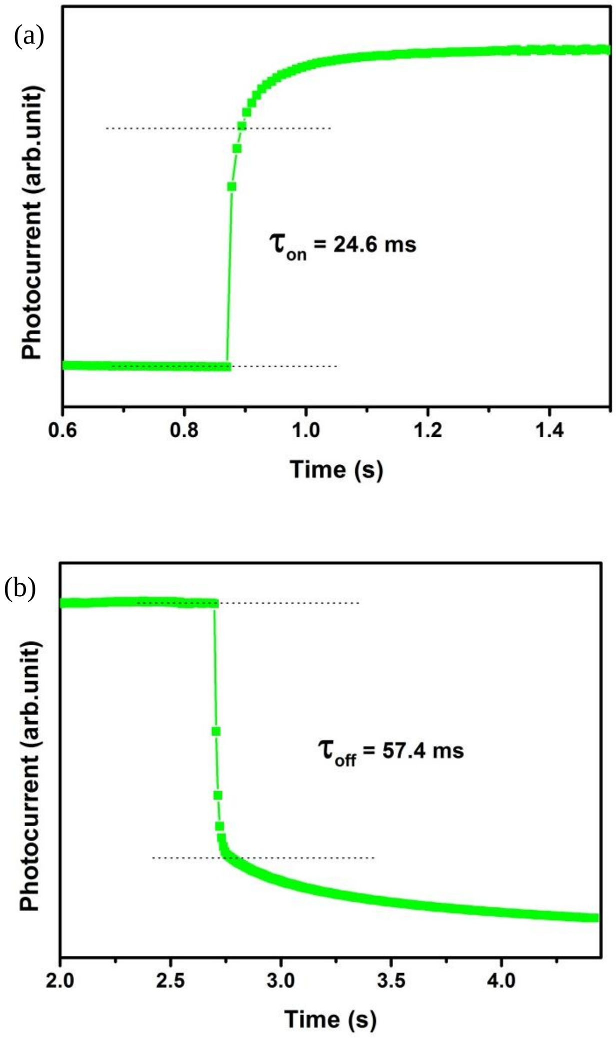

Figure S9. I-V curves of four contacts (left) indicating the successful contact of four electrodes on the In_2Se_3 film. Final Hall results of the multilayer In_2Se_3 film measured at room temperature (right) revealing an n-type behavior with mobility (μ) of 76.8 cm^2 /Vs.

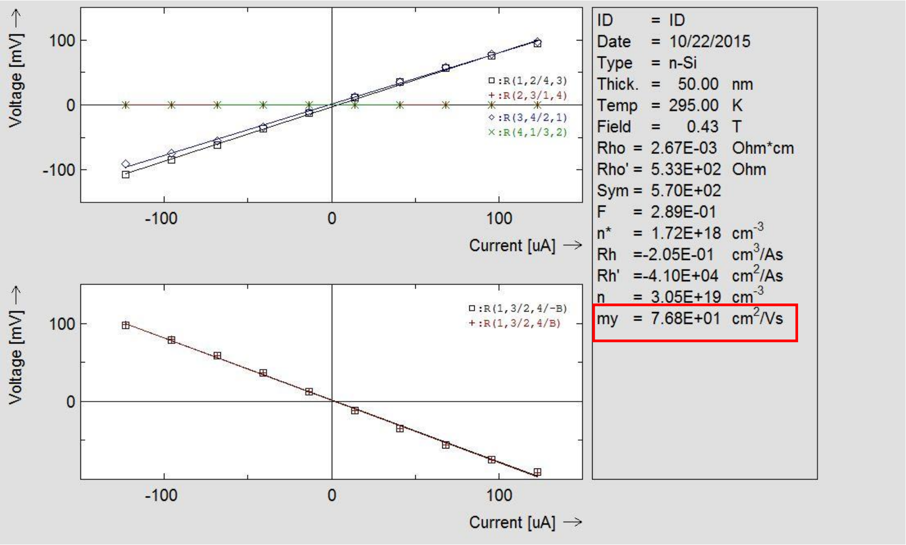

ID = ID
Date = 10/22/2015
Type = n-Si
Thick. = 50.00 nm
Temp = 295.00 K
Field = 0.43 T
Rho = 2.67E-03 Ohm*cm
Rho' = 5.33E+02 Ohm
Sym = 5.70E+02
F = 2.89E-01
n* = 1.72E+18 cm^{-3}
Rh =-2.05E-01 cm^3/As
Rh' =-4.10E+04 cm^2/As
n = 3.05E+19 cm^{-3}
my = 7.68E+01 cm^2/Vs

Figure S10. (a) I-V curves under ambient and vacuum conditions. Light power density: 20 mW/cm^2. (b) Temporal photoresponse of the In_2Se_3 device at V_{ds} = 0.2 V.

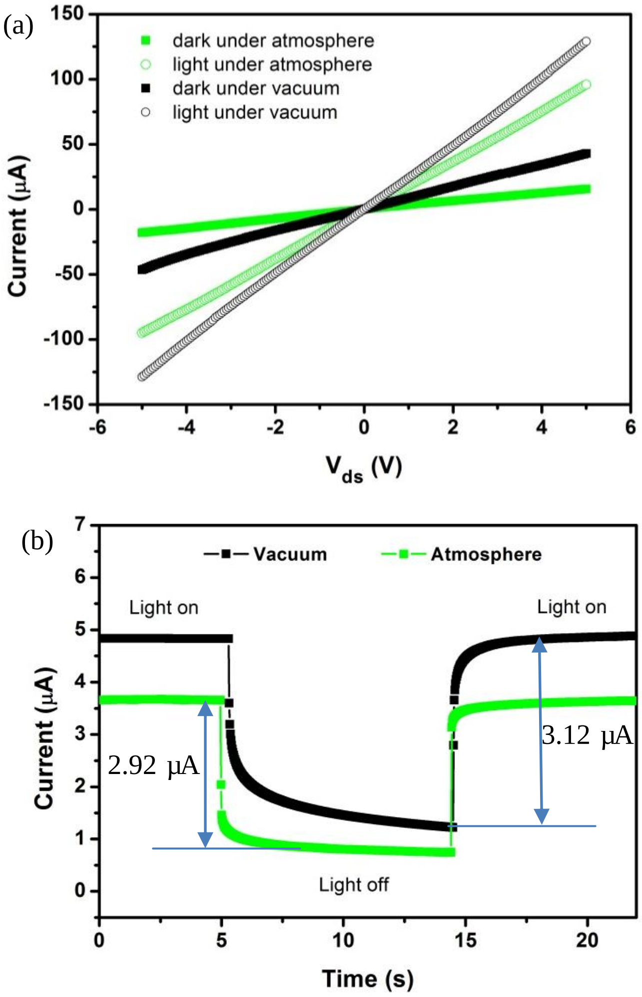

Figure S11. The In_2Se_3 film deposited on the conventional SiO_2/Si substrate and its corresponding optoelectronic properties. (a) The optical images of the deposited In_2Se_3 film (green part). (b) I-V characteristics of the In_2Se_3 photodetector in the presence and absence of light (λ = 532 nm, power density = 20 mW/cm^2). (c) Time-dependent switching behavior of the photodetector under 0.2 V bias voltage. (d) Illumination intensity dependent photocurrent (black squares) and responsivity (blue squares) at V_{ds} = 5 V. The power laws of $I_{ph} \sim P^{0.453}$ was calculated from fitting the measured photocurrents.

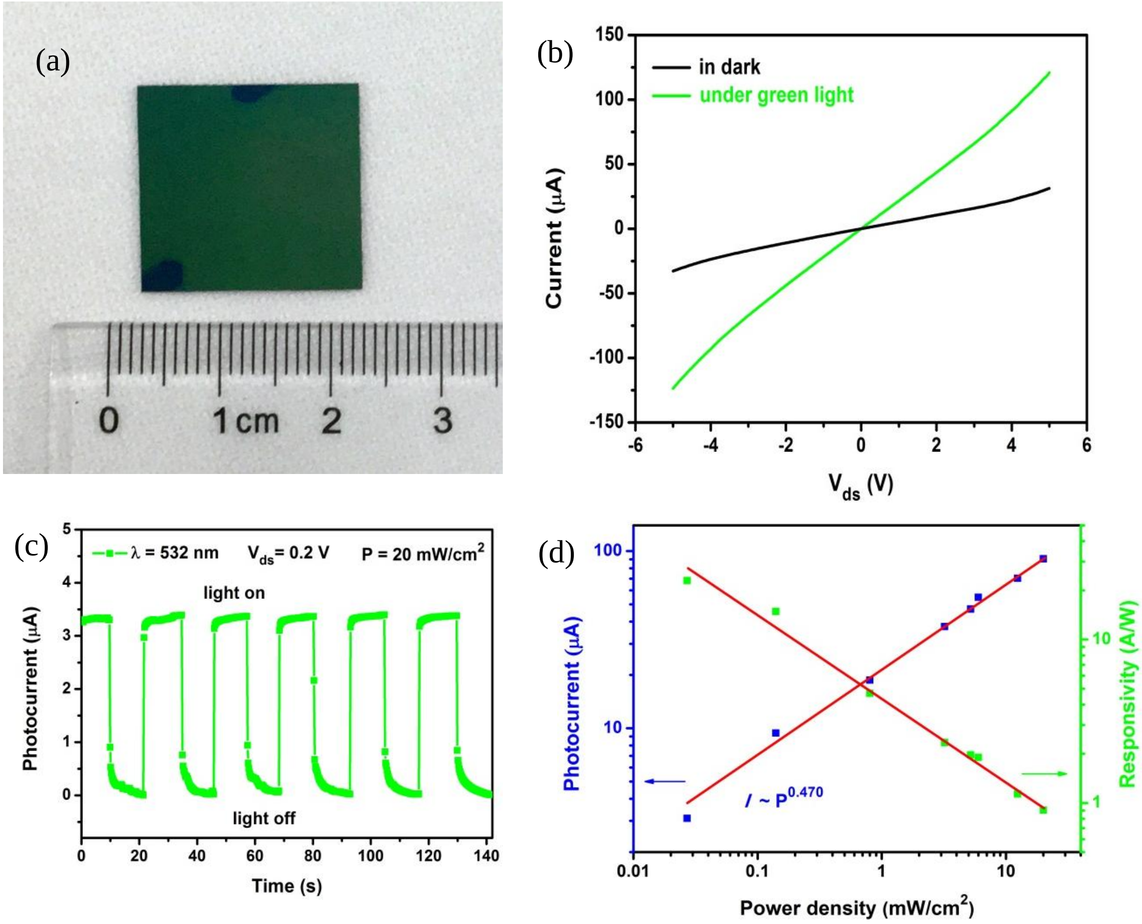

Figure S12. The In_2Se_3 film deposited on the commercial PI substrate and its corresponding optoelectronic properties. (a) The optical images of the deposited In_2Se_3 film (white part). The inset is in a flexed state. (b) I-V characteristics of the In_2Se_3 photodetector in the presence and absence of light (λ = 532 nm, power density = 20 mW/cm^2). (c) Time-dependent switching behavior of the photodetector under 0.2 V bias voltage. (d) Illumination intensity dependent photocurrent (black squares) and responsivity (blue squares) at V_{ds} = 5 V. The power laws of $I_{ph} \sim P^{0.471}$ was calculated from fitting the measured photocurrents.

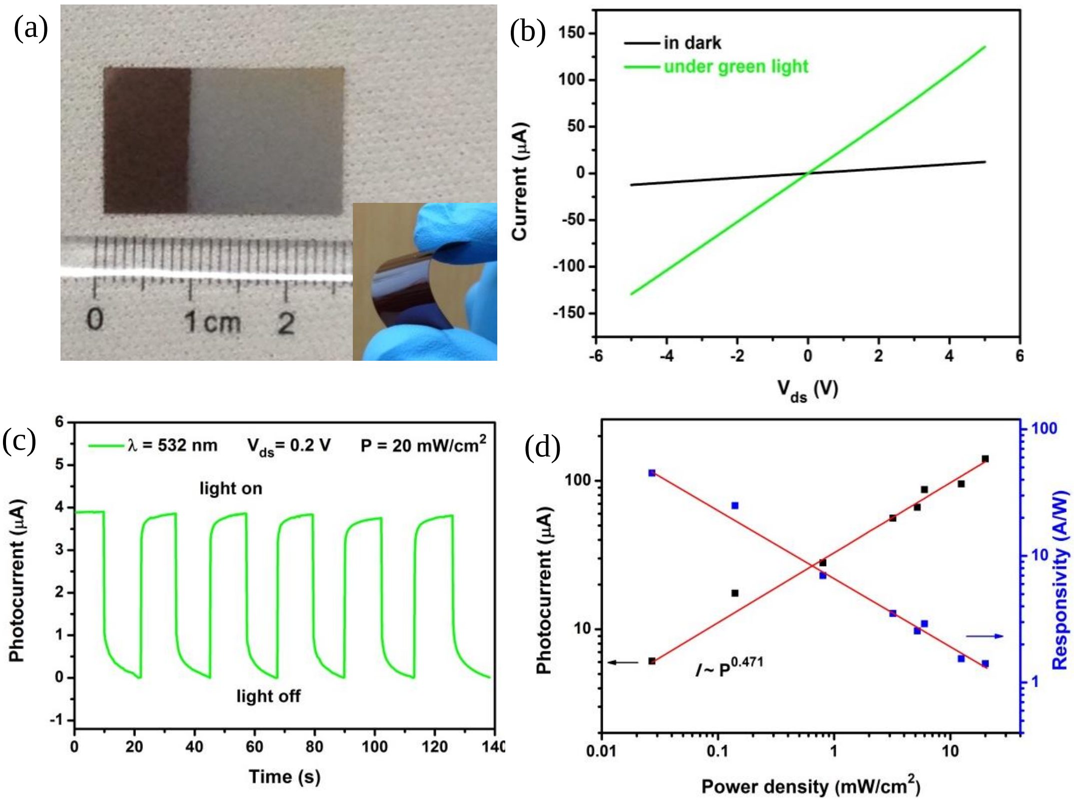

Figure S13. The In_2Se_3 film deposited on transparent sapphire substrate and its corresponding optoelectronic properties. (a) The optical images of the deposited In_2Se_3 film. Its transparency is revealed by the visibility of the flower placed beneath the transparent devices. (b) I-V characteristics of the In_2Se_3 photodetector in the presence and absence of light (λ = 532 nm, power density = 20 mW/cm^2). (c) Time-dependent switching behavior of the photodetector under 0.2 V bias voltage. (d) Illumination intensity dependent photocurrent (black squares) and responsivity (blue squares) at V_{ds} = 5 V. The power laws of $I_{ph} \sim P^{0.453}$ was calculated from fitting the measured photocurrents.

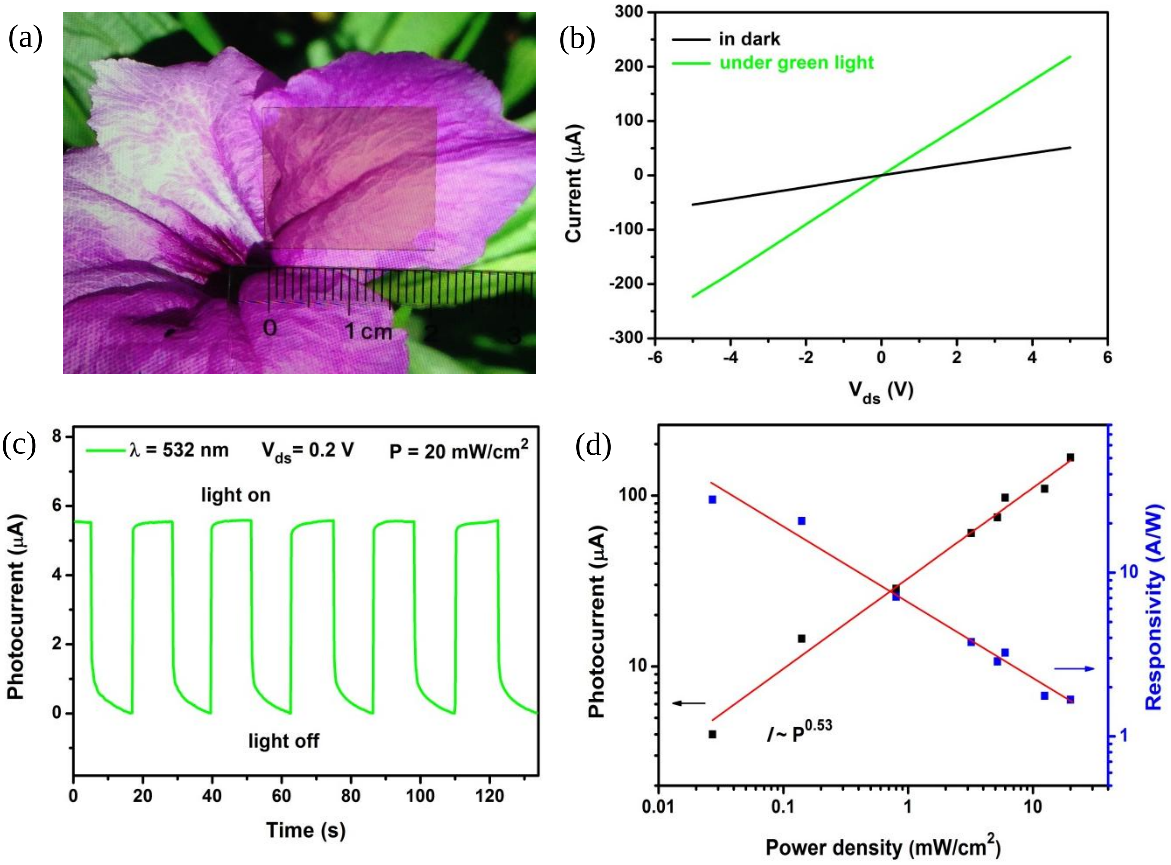

References

1. S. H. Yu, Y. Lee, S. K. Jang, J. Kang, J. Jeon, C. Lee, J. Y. Lee, H. Kim, E. Hwang and S. Lee, *ACS Nano*, 2014, **8**, 8285-8291.
2. Z. Yin, H. Li, H. Li, L. Jiang, Y. Shi, Y. Sun, G. Lu, Q. Zhang, X. Chen and H. Zhang, *ACS Nano*, 2011, **6**, 74-80.
3. W. Choi, M. Y. Cho, A. Konar, J. H. Lee, G. B. Cha, S. C. Hong, S. Kim, J. Kim, D. Jena, J. Joo and S. Kim, *Adv. Mater.*, 2012, **24**, 5832-5836.
4. F. Xia, T. Mueller, Y. M. Lin, A. Valdes-Garcia and P. Avouris, *Nat. Nanotechnol.*, 2009, **4**, 839-843.
5. P. Hu, Z. Wen, L. Wang, P. Tan and K. Xiao, *ACS Nano*, 2012, **6**, 5988-5994.
6. J. D. Yao, Z. Q. Zheng, J. M. Shao and G. W. Yang, *Nanoscale*, 2015, **7**, 14974-14981.
7. J. Xia, X. Huang, L.-Z. Liu, M. Wang, L. Wang, B. Huang, D.-D. Zhu, J.-J. Li, C.-Z. Gu and X.-M. Meng, *Nanoscale*, 2014, **6**, 8949-8955.
8. J. Lu, A. Carvalho, X. K. Chan, H. Liu, B. Liu, E. S. Tok, K. P. Loh, A. H. Castro Neto and C. H. Sow, *Nano Lett.*, 2015, **15**, 3524-3532.
9. P. Hu, L. Wang, M. Yoon, J. Zhang, W. Feng, X. Wang, Z. Wen, J. C. Idrobo, Y. Miyamoto, D. B. Geohegan and K. Xiao, *Nano Lett.*, 2013, **13**, 1649-1654.
10. S. R. Tamalampudi, Y. Y. Lu, U. R. Kumar, R. Sankar, C. D. Liao, B. K. Moorthy, C. H. Cheng, F. C. Chou and Y. T. Chen, *Nano Lett.*, 2014, **14**, 2800-2806.
11. M. S. Choi, D. Qu, D. Lee, X. Liu, K. Watanabe, T. Taniguchi and W. J. Yoo, *ACS Nano*, 2014, **8**, 9332-9340.
12. R. B. Jacobs-Gedrim, M. Shanmugam, N. Jain, C. A. Durcan, M. T. Murphy, T. M. Murray, R. J. Matyi, R. L. Moore, 2nd and B. Yu, *ACS Nano*, 2014, **8**, 514-521.
13. M. Lin, D. Wu, Y. Zhou, W. Huang, W. Jiang, W. Zheng, S. Zhao, C. Jin, Y. Guo, H. Peng and Z. Liu, *J. Am. Chem. Soc.*, 2013, **135**, 13274-13277.
14. Q. L. Li, C. H. Liu, Y. T. Nie, W. H. Chen, X. Gao, X. H. Sun and S. D. Wang, *Nanoscale*, 2014, **6**, 14538-14542.
15. Q. Wang, K. Xu, Z. Wang, F. Wang, Y. Huang, M. Safdar, X. Zhan, F. Wang, Z. Cheng and J. He, *Nano Lett.*, 2015, **15**, 1183-1189.
16. Z. Wang, M. Safdar, M. Mirza, K. Xu, Q. Wang, Y. Huang, F. Wang, X. Zhan and J. He, *Nanoscale*, 2015, **7**, 7252-7258.
17. Y. Zhou, Y. Nie, Y. Liu, K. Yan, J. Hong, C. Jin, Y. Zhou, J. Yin, Z. Liu and H. Peng, *ACS Nano*, 2014, **8**, 1485-1490.